

Synthesis and Mechanical Studies of Mg-Hydroxyapatite Composite for Biomaterials Applications

Atul Kumar Maurya

A Dissertation Submitted to
Indian Institute of Technology Hyderabad
In Partial Fulfilment of the Requirements for
The Degree of Master of Technology



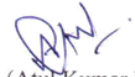
भारतीय प्रौद्योगिकी संस्थान हैदराबाद
Indian Institute of Technology Hyderabad

Department of Material Science and Metallurgical Engineering

June, 2015

Declaration

I declare that this written submission represents my ideas in my own words, and where others' ideas or words have been included, I have adequately cited and referenced the original sources. I also declare that I have adhered to all principles of academic honesty and integrity and have not misrepresented or fabricated or falsified any idea/data/fact/source in my submission. I understand that any violation of the above will be a cause for disciplinary action by the Institute and can also evoke penal action from the sources that have thus not been properly cited, or from whom proper permission has not been taken when needed.

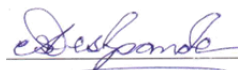


(Atul Kumar Maurya)

(ms13m1003)

Approval Sheet

This thesis entitled “Synthesis and Mechanical behavior of Mg-Hydroxyapatite composite for biomaterial applications” by Atul Kumar Maurya is approved for the degree of Master of Technology from IIT Hyderabad.



Dr. Atul Suresh Deshpande

Assistant Professor

Department of Materials Science and Metallurgical Engineering

Adviser



Dr. Bharat Bhooshan Panigrahi

Assistant Professor

Department of Materials Science and Metallurgical Engineering

Co-Guide

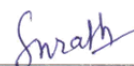


Dr. Ranjith Ramadurai

Assistant Professor

Department of Materials Science and Metallurgical Engineering

Examiner



Dr. Subha Narayan Rath

Assistant Professor

Department of Biomedical Engineering

Chairman

Acknowledgements

I wish to express my deep sense of gratitude and indebtedness to **Dr. Atul Suresh Deshpande**, Department of Material Science and Metallurgical Engineering, I.I.T Hyderabad for assigning me the project “Synthesis and degradation studies of Mg-hydroxyapatite composite for biomaterials applications” and for his inspiring guidance, constructive criticism and valuable suggestion throughout this project work.

I would like to express my gratitude to **Dr. Bharat Bhooshan Panigrahi, Dr. Subha Narayan Rath and Dr. Mudrika Khandelwal** for their valuable suggestions and encouragements at various stages of the work.

I am also thankful to **Mr. Damodar Devrakonda, Mr. Anand Kumar Mak, Mrs. Usha Rani** and other research scholars in Department of Material Science and Metallurgical Engineering for providing all joyful environments in the lab and helping me throughout this project.

Last but not least, my sincere thanks to all my friends who have patiently extended all sorts of help for accomplishing this undertaking.

Atul Kumar Maurya
M.Tech
Material Science and
Metallurgical Engineering

Dedicated
to
My Family

ABSTRACT

Last few decades has seen enormous growth in terms of bone replacement materials. Relying on their desirable mechanical properties (strength and toughness), metallic materials such as stainless steel and titanium based alloys have been widely used for the application of bone fixation (replacement). However, these materials have their own limitations. For example, high modulus of elasticity of steel and titanium alloys can lead to bone atrophy, they have good corrosion resistance but wear followed by corrosion may lead to release of toxic ions in the body. Alternatively, ceramic, polymeric and composite materials have been tried as bone replacement materials. In recent years the research focus is shifted to using bioresorbable materials as bone replacement. In this regards, magnesium based implants have been investigated extensively. Magnesium metal has moderate elastic modulus and density similar to that of bone. In aqueous environment it dissolves. These properties make magnesium metal an ideal material for bioresorbable bone implant material. Yet their use is impeded by two major hurdle. One, pure magnesium dissolves rapidly so rapid loss in mechanical properties occur. Secondly, hydrogen gas evolved during the degradation gets accumulated in tissue surrounding the implant. Extensively research is going on to control degradation behaviour of magnesium through alloying and coating with non-degradable bio-ceramics.

The main objective of this study is to synthesize magnesium- hydroxyapatite (Mg-HAP) composites and assess the effect of morphology of hydroxyapatite (HAP) scaffolds on mechanical and structural behaviour of magnesium-hydroxyapatite composite (MMC). By controlling the pore sizes of HAP scaffold, we expect to control surface area for cell growth and degradation rate of magnesium metal. Mg-HAP metal-ceramic composite can serve two purposes. It may be able to control the degradation rate of magnesium metal. Secondly, as the magnesium metal dissolves the porous HAP scaffold can support tissue in growth and provide mechanical strength at the same time.

For the synthesis of hydroxyapatite, monobasic phosphate was tried. However end product was not in phase to HAP standard XRD patterns. It was mixture of DCP, HAP and Calcium hydrogen phosphate. No or very less phases of HAP was formed by using monobasic phosphate. To get phase of HAP we changed the precursor from monobasic phosphate to dibasic phosphate. We also changed mode of addition of the solutions in co-precipitation method, to see the effect on hydroxyapatite powder.

To synthesize slurry for coating over PU foam many solvents (water and acetone) were tried with PVA (binder). Due to bubble formation during coating, solvents were replaced. So a mixture of water/alcohol (50:50) by volume was ideal for slurry. Prepared slurry were coated over two types of foam having range 30 ppi and 60 ppi. Coated sample was dried and sintered at 1000 °C to get HAP scaffold. Phase purity of the sintered HAP was confirmed by XRD. FESEM and Optical Microscope

was used to check interconnectivity and thickness of the pores and wall respectively. Compressive strength of the scaffold was tested on Universal Testing Machine (UTM). Adipose derived stem cell (ADSC) was used for in vitro cell culture studies. FDA/PI solution was used to check cells are alive or dead in vitro medium with scaffolds. Images were taken by florescence microscopy.

Magnesium powder was used for impinging magnesium into scaffold to get Mg-HAP composite. Phase purity of the magnesium powder after and before melting was characterized by XRD and DSC. Here we attempted melt-cast route to impinge magnesium in HAP scaffold.

Nomenclature

$\text{Ca}(\text{NO}_3)_2 \cdot 4\text{H}_2\text{O}$ -Calcium Nitrate Tetra hydrate

$\text{NH}_4\text{H}_2\text{PO}_4$ - Ammonium dihydrogen Phosphate

$(\text{NH}_4)_2\text{HPO}_4$ -Di-ammonium Hydrogen Phosphate

NH_4OH -Ammonium Hydroxide

Mg-Magnesium

HAP-Hydroxyapatite

DCP-Di Calcium Phosphate

TCP-Tri Calcium Phosphate

PU-Polyurethane Foam

ppi- Pores per inch

XRD-X-Ray Diffraction

DSC-Differential Scanning Calorimetry

SEM-Scanning Electron Microscopy

Contents

Declaration	2
Approval Sheet	3
Acknowledgements	4
Abstract	5
Nomenclature	7
1 Introduction.....	10
1.1 Metallic Implant	10
1.2 Ceramic Implant.....	10
1.3 Polymeric Implant	11
1.4 Composite Materials.....	12
1.5 Bioresorbable Material	12
1.6 Hydroxyapatite-Mg composite.....	13
2 Literature Review	14
2.1 Literature Review on HAP Synthesis.....	14
2.2. Literature Review on Scaffold Synthesis	15
2.3 Literature Review on Bioresorbable Materials.....	16
2.4 Objectives.....	17
3 Experimental Details	18
3.1 Synthesis and optimization of HAP nano powder by co-precipitation method.....	18
3.2 Preparation and optimization of slurry.....	21
3.3 Processing of porous HAP scaffold through Polymeric sponge method.....	21
3.4 Mg-HAP composite preparation by melt casting of magnesium powder.....	23
3.5 Characterization.....	23
3.5.1 Phase analysis of HAP, Sintered HAP and Magnesium by XRD.....	23
3.5.2 Density and Porosity measurement.....	24
3.5.3 Measurement of Wall thickness and Pore diameter.....	24
3.5.4 Measurement of compressive strength.....	25
3.5.5 Microstructure analysis of scaffold by SEM.....	25
3.5.6 DSC of magnesium and heat treated magnesium.....	25
3.5.7 Cell culture test of scaffold.....	25
4 Result and Discussion	26

4.1 Phase analysis of HAP after synthesis.....	26
4.2 Phase analysis of HAP after sintering.....	28
4.3 Phase and DSC analysis of Mg before and after heat treatment.....	29
4.4 Density and porosity measurement.....	31
4.5 Wall thickness and microstructure(SEM).....	31
4.6 Compressive strength.....	36
4.7 Cell culture test.....	37
5 Conclusion	39
References.....	41

CHAPTER 1

INTRODUCTION

Human skeleton is composed of hard tissue called bone and flexible cartilaginous tissue which provides support and allows flexible movement of body. Bones are mainly composed of hydroxyapatite $[\text{Ca}_{10}(\text{PO}_4)_6(\text{OH})_2]$ crystal deposited on an organic matrix (collagen)[1]. Porosity of natural bone varies from 50% to 90%. Four cell types are present in bone tissue: osteoblasts, osteoclasts, osteocytes and bone lining cells. Bone is in a constant state of remodelling with osteoblasts producing and mineralizing new bone matrix, osteocytes maintaining the matrix and osteoclasts resorbing the matrix. Bone lining cells are inactive cells that are believed to be precursors for osteoblasts [1]. This constant remodelling process can eliminate micro cracks and defect in bone resulting from external mechanical stimuli and body movements. However, in case of compound fracture or any bone related disease they may get damaged beyond repair by regular remodelling process. This necessitates artificial replacement of bone tissue by an implant. The material which is used in these applications must be non-toxic to the body and at the same time it should be biocompatible with respect to surrounding tissue. A material which satisfies these criteria is called biomaterial. In general terms, bio-materials are defined as nonviable materials used in a medical device, intended to interact with biological systems. Alternatively, biomaterials are the materials that serve as replacement of body part or function of a body part in a safe, economic, reliable and physiologically accepted manner. Basically these bio-materials classified into four broad categories, 1). Metallic, 2). Ceramics, 3). Polymers and 4). Composites. Among these metallic bio-materials are widely being used in hip and knee replacements, since they possess good mechanical properties and fracture toughness as well.

1.1 Metallic Implant materials:

Metal implants in the form of wire, bands, screws, bolts, staples, nails and plates are applied in the temporary fixation of fractures. Common use of metals for as implant materials is as old as 1900s. Demand for metallic bone replacement implants is very high, especially hip and knee replacement implants. Metals and metal alloys such as stainless steel, titanium alloy are known for high strength, ductility and resistance to wear. However, metallic materials also exhibit certain problems such as low biocompatibility, wear induced corrosion and mechanical property mismatch. For example, cobalt-chromium alloys are known for high corrosion resistance, however, it has been reported that the tissue surrounding the cobalt-chromium alloys implant was stained green or grey and surrounded with

a paste-like material. Joint fluid tests revealed high levels of cobalt [2], which are the effect of metallosis and metal poisoning. High stiffness of metals compared to surrounding tissue (bone) results in stress shielding effect causing bone atrophy. This may lead to loosening of implant or stress induced fracture of bone surrounding the implant. Many types of strategies have been employed to address these issues such as ceramic coating to improve biocompatibility and improve corrosion resistance. Create porosity in implant body to reduce mechanical mismatch and to allow native bone growth for better osteointegration [3].

1.2 Ceramic Implant material:

Ceramics such as alumina and toughened zirconia are the most recent materials used for hip implants [4]. They have excellent bio-compatibility and corrosion resistance. They also have good wear resistance and high mechanical strength compared to polymers. However problem with ceramics is that they are very brittle. So they cannot be used for load bearing applications. Hydroxyapatite [$\text{Ca}_{10}(\text{PO}_4)_3(\text{OH})_2$] is one of the most bio-compatible materials for bone replacement. It has chemical and physical resemblance with natural bone mineral. It is bioactive ceramic widely used as powder or particulate forms in various bone repairs and coating materials for metallic prostheses to improve their biological properties. It has excellent biocompatibility, bioactivity and osteoconductivity. HAP is most stable near to the pH, temperature and composition to the physiological fluid.

The necessity of porous structure in bone regeneration is also important as porous structure helps in growth of new bone tissue. Reports show that no new bone formed on solid particles where as in porous structure directly osteogenesis occurred [5]. Porous scaffolds are key component in bone regeneration which serves as a template for cell interactions and formation of bone-extracellular matrix to provide structural support to the newly formed tissue. Scaffolds for this purpose should meet certain criteria to serve this function including mechanical, biocompatibility and biodegradability. However the problem with this scaffold is that they don't have good mechanical strength.

1.3 Polymers:

Polymer materials used in hip implant have been under improvements and research since 50 year. Currently we are getting successful replacement with 90 % survival rate after 10 year in vivo. Ultra-High-Molecular-Weight Polyethylene (UHMWPE) can be used against cobalt-chromium alloy and ceramic implants [6]. Polymers have good wear resistance property than metallic and ceramic implants. Due to less wear resistance of polymers they start bone lesions that can compromise the implant. Crosslinking of UHMWPE has been shown to reduce the volume of evolved particles.

1.4 Composite:

The basic requirements for human joints include mechanical property (yield stress, plasticity, Young's Modulus, Fatigue strength), physical properties (density, magnetic properties etc.). Conventional replacements have some drawbacks like metallosis and metal poisoning, brittleness in ceramic and bone-lesions in polymers. With the help composite material we can solve these problems. Properties of composites depend upon, composition, structural and physical properties of individual components (matrix and dispersed phase) and distribution of dispersed phase. Thus by changing one or more of these parameters, physical properties of composites can be fine-tuned. To get a metal free implant researchers have used carbon fibre reinforced PEEK for hip implant [7]. This composite have high strength with biocompatible polymer composite. Metal matrixes with fibre reinforced composites have been used these days due to their high strength, durability and biocompatibility [8]. However if we can use one component as biodegradable materials with ceramics they may give better property than current composite materials. As if one component comes out then we will have again natural tissue instead of synthetic in the body.

1.5 Bioresorbable Materials:

Materials which degrade under physiological condition (*in vivo*) are termed as bioresorbable materials. Typically these materials degrade and degradation products are taken up by surrounding tissue or transported through circulatory systems to excretory organs [9]. Multiple biological and chemical mechanisms are involved during material desorption which dictate the rate of resorption. Thus for using bioresorbable of implant applications, we must keep in mind that the degradation rate and tissue/cell growth must match in order to allow proper tissue regrowth. So far the use of bioresorbable materials in clinical use is dominated by polymer such as poly lactic acid (PLA), polyglycolic acid (PGA) poly caprolactones etc. and their combinations [10], recent years has seen use of metallic materials for stents, and fracture fixation. Among metallic materials magnesium based materials are the most explored candidate [11] other less explored metals include iron and zinc etc.

1.6 Hydroxyapatite (HAP)-Mg composite:

As discussed before about the control over degradation rate. So study of this composite is to get a composite which can be taken as long last. As we know that if we can make outer surface of the pore size smaller as possible (not less than 100 μm) then magnesium will get less area to react. Hence ultimately we are decreasing their degradation rate. Hydroxyapatite is also very similar to bone structure and they have excellent biocompatible. In this study we will focus on the comparative strength of the composite with pure magnesium. We will try to use less amount of HAP comparable to magnesium. We will try to form a scaffold of Hydroxyapatite-Magnesium composite with pore size not less than 100 μm . Here in this composite magnesium will come out through exertion after completing their objective, whereas hydroxyapatite will remain as ceramic. We will study mechanical

and other properties of the composite. First we will form a template of the hydroxyapatite of pore size not less than 100 μm . Keep in mind pores should be interconnected as body fluid and bone tissue will grow later. Now we will try to incorporate magnesium inside these pores. So as after some time magnesium will come out and we will have a new formed bone tissue with hydroxyapatite. As we know that aim of this project is only to study mechanical behaviour of hydroxyapatite-Mg composite. So we will not bother about chemical and other properties. The only thing what we are searching here is strength with bioresorbable material. However as HAP is not a bioresorbable material but it has excellent biocompatible properties. Main objective of this study is to provide a hip implant material with maximum percentage of natural bone tissue.

CHAPTER 2

Literature Review

The main objective of our work was to fabricate Mg-HAP composite. Since the melting temperature of pure Mg is far less than temperature necessary for sintering of HAP we decided to follow a two-step process. In the first step, HAP scaffolds were prepared dip-coating of PU foams followed by sintering. For effective sintering it is essential that the starting powders with small and uniform particle size. Numerous literature reports have explored the synthesis of hydroxyapatite and the effect of preparation conditions on morphology and phase formation of HAP.

2.1 Literature Review on HAP synthesis:

A.Cuneyt Tas et. al [12] studied the synthesis of biomimetic synthetic HAP powder at 37 °C in synthetic body fluid. Hydroxyapatite (HAP, $\text{Ca}_{10}(\text{PO}_4)_6(\text{OH})_2$), was prepared as a nano-sized (~50nm), homogeneous and high-purity ceramic powder from calcium nitrate tetrahydrate and diammonium hydrogen phosphate salts. Palanivelu. R and A. Mary Saral et. al [13] studied the role of pH during the synthesis of hydroxyapatite powder by using calcium nitrate tetrahydrate and diammonium hydrogen phosphate as starting material through co-precipitation method. They studied the result under various pH conditions 7, 9 and 11. X-Ray diffraction technique was used to check crystallinity of the powder. Result revealed that presence of nanocrystallinity HAP at pH above 8.

2.2 Literature Review on scaffold synthesis:

Soon-Ho kwol et al. [14] fabricated porous bioceramics with variable porosity using polyurethane foam technique. Porosity was controlled by number of coatings on the PU foam struts. When a single coated scaffold was measured it was showing porosity up to 90% and pores were completely interconnected. Whereas when sintered scaffold was coated 5 to 6 times again they were showing porosity of 60%. Compressive strength was strongly dependent on porosity not on type of ceramic HA, TCP or HA/TCP composite.

I. Sopyan et al. [15] studied on porous hydroxyapatite for artificial bone applications. It was reported that the preparation of HAP porous bodies via polymeric sponge method; the samples which were prepared using sol-gel method-derived HA powders and commercial HAP powders showed a considerable compressive strength ranging from 1.3 to 10.5MPa for the increased apparent density from 1.27 to 2.01 g/cm³. This is higher than the 0.55–5MPa compressive strength obtained for the apparent densities of 0.0397– 0.783 g/cm³, as reported by Ramay et al. [16]. The porous HAP showed macro pores of 400–600 μm diameters with good pore interconnecting channels. It was also shown

that homogeneity of slurry and heating rate affected porosity and density of porous bodies, in turn influencing the compressive strength. More homogeneous slurries and faster heating rate gave porous bodies with the increased compressive strength due to higher apparent density and crystallinity.

Vassilis Karageorgiou and David Kaplan [17] studied the porosity of 3D biomaterial scaffolds and osteogenesis. It has been seen that porosity and pore size of biomaterial scaffolds play a critical role in bone formation in-vitro and in-vivo. This review explores the state of knowledge regarding the relationship between porosity and pore size of biomaterials used for bone regeneration. The effect of these morphological features on osteogenesis in-vitro and in-vivo, as well as relationships to mechanical properties of the scaffolds, is addressed. In-vitro, lower porosity stimulates osteogenesis by suppressing cell proliferation and forcing cell aggregation. In contrast, in-vivo, higher porosity and pore size result in greater bone ingrowth. The minimum requirement for pore size is considered to be ~100 μm due to cell size, migration requirements and transport. However, pore sizes ~300 μm are recommended, due to enhanced new bone formation and the formation of capillaries.

Schwartzwalder and Somers et al. [18] successfully produced porous structure of scaffold by using slurry infiltration process. In this process foam was infiltrated with ceramic slurry and body was compressed by passing it through the sets of rollers to remove excess slurry. In this process slurry remained coated over struts and open pore channel were remain in between. Template was then dried followed by burning of PU foam and sintering at higher temperature. The structure, which was produced that have porous structure with open channel in it.

2.3 Literature Review on Bioresorbable Material:

As search from literature polymers have adverse reactions to body fluids. Metals are more promising compare to polymer as they have good mechanical strength and properties resembles with natural bone. If we compare to Fe and Mg then magnesium takes less time in degradation than iron hence Magnesium is the best material for our composite. As they also have very less resistance to corrosion in wet environment [9]. So if we look for perfect bioresorbable materials which have strength as well as good control over degradation rate then magnesium is only answer. We can also use as bone screw or plate after a certain span of time they get absorb. However main problem associated with magnesium that is they have very high degradation rate. They degrade before the sufficient healing of the new formed bone tissue takes place. So ultimately they are leaving there mission by not providing support for up to sufficient healing of bone tissue over matrix. Hence implant must get enough time for their support from the natural tissue and cells before magnesium degrades. During degradation of magnesium they also produce hydrogen which is toxic for our body. However as we know that slow rate of degradation that is up to some limit our body can tolerate. So in present days the problem with magnesium is its rapid degradation rate which prevents its clinical application so vast. Hence its rapid degradation time is hampering its acceptance. Localized formed hydrogen also accumulate around the implant and they delay the healing of the tissue. Localized

formed hydrogen also increases the pH of the system which is danger for the body known as alkalization which affects body physiological process. To give enough time to the cells and tissues for healing the fractured part we have to give enough time to them before resorbable material compromise. Tissues and cells wants to give their own support over matrix and this is possible when time span of degradation rate is enough. However these day surface modification and alloy technology have been used to slow down its degradation rate. Hence ultimately controlled degradation rate will produce a controlled amount of hydrogen which is easily absorbed by body. So magnesium can be used after surface treatment and alloying as a bioresorbable material with a fixed expiration date. We can control the degradation rate by three famous techniques as Magnesium purification, selective Alloying and Anodized coating. Cadmium (Cd), Manganese (Mn), tin (Sn), Zinc (Zn) and Calcium (Ca) have mild effect on the corrosion rate of Mg with their efficacy being dependent on solute concentration. Alloy of Ca-Mg-Zn is one of the good examples. In which calcium provides corrosion resistance and zinc provides strength to the material. Hence by alloying are anodizing (control degradation) the magnesium we can easily use magnesium as a bioresorbable material.

X.N. Gu et al. [19] studied about the biocompatibility of the magnesium material due to their excellent mechanical property and pore similarity to natural bone. Porous structure provides opportunity for invasion of the cells, formation of blood vessels and eventually replacement of newly formed bone after gradual degradation and absorption of the magnesium ion.

B.Denkena et al.[20] found that magnesium material offers great absorbable potential as implant materials. They degrade within a certain time span after surgery and therefore are suitable for temporary implant to accomplish medical function. These implants support fracture until healing, as conventional metals are too stiff hence leading to impairment of healing process and normal stress.

Harpreet S. brar et al. [9] concluded that need for structural materials in temporary implant applications has grown, materials that provide short-term structural support and can be reabsorbed into the body after healing are being sought. As traditional metallic materials were bio-compatible but they were not bioresorbable hence in the bio-medical field interest grown up towards bio-resorbable materials.

2.4 Objective of present study:

- To synthesize nanopowders of hydroxyapatite ($\text{Ca}_{10}(\text{PO}_4)_6\text{OH}_2$) with uniform particle size.
- To form a scaffold of porous hydroxyapatite using open pore polyurethane foams with varying pore size (100-500 μm) as templates.
- Study of porosity, bulk density, compressive strength, pore size, pore size distribution and microstructure of porous HAP scaffolds by varying solid loading, binder contents, amount and size of pore former.

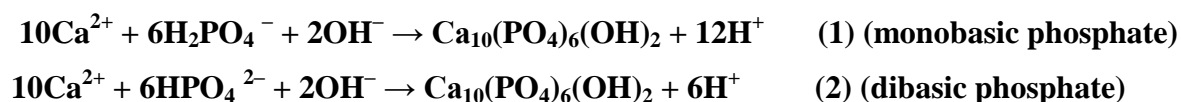
- Incorporating magnesium in the pores of scaffolds by melt casting to get HAP-Mg composite material.

CHAPTER 3

Experimental

3.1 Synthesis and optimization of HAP nano powder by co-precipitation method:

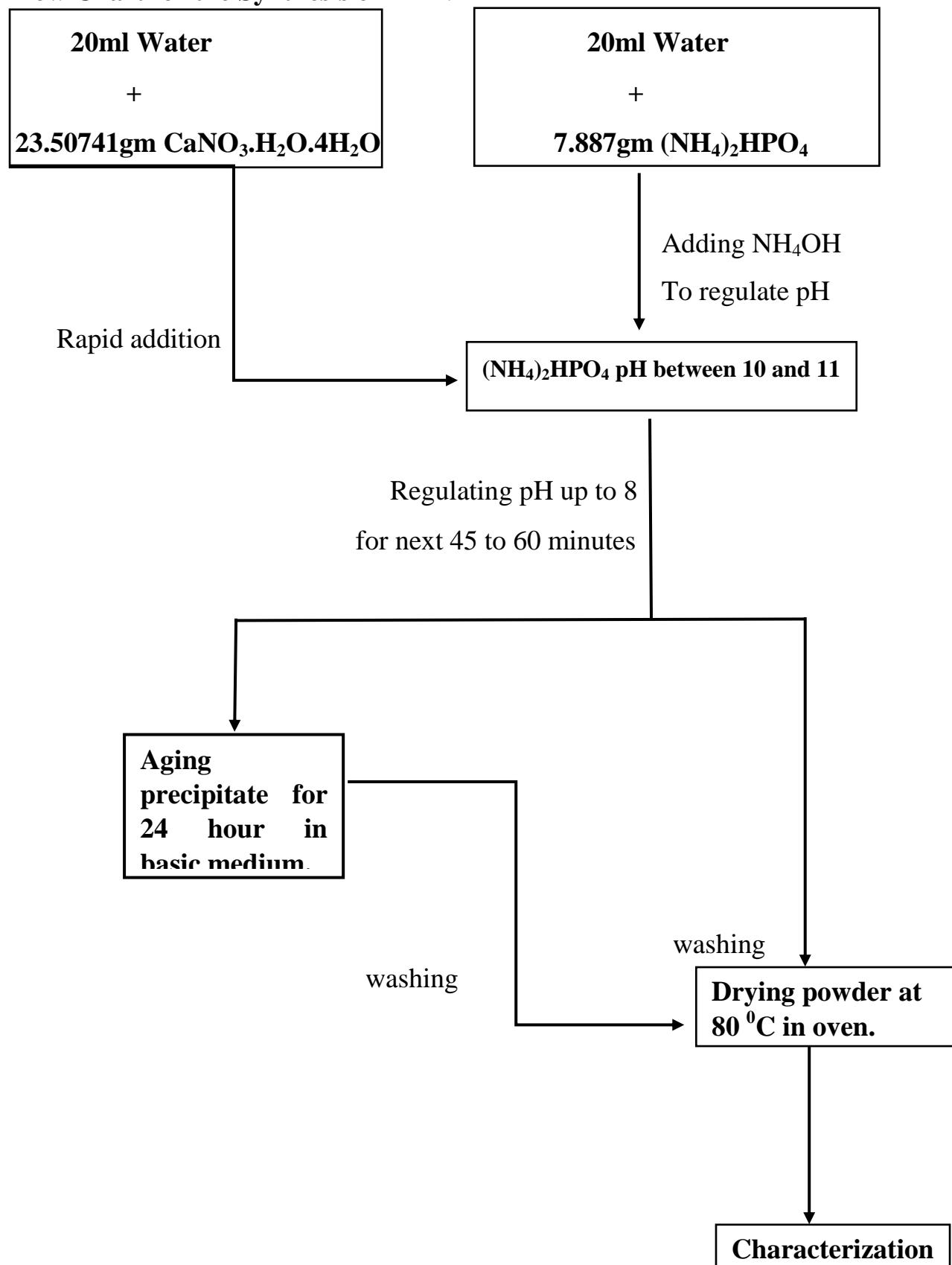
Synthesis of hydroxyapatite was carried out using two different precursors. While most of the HAP synthesis processes reported in the literature have been carried out using dibasic phosphates or phosphoric acid as phosphate precursor, there are no reports on the use on monobasic phosphate precursor for synthesis of HAP. In the work we synthesized HAP using both monobasic and dibasic phosphate precursors in order to study the effect of precursor on phase formation of HAP. The reagents used for HAP synthesis were calcium nitrate tetrahydrate $[\text{Ca}(\text{NO}_3)_2 \cdot 4\text{H}_2\text{O}]$ (Sigma-Aldrich) (99%), ammonium dihydrogen phosphate $[\text{NH}_4\text{H}_2\text{PO}_4]$ (Sigma-Aldrich) (99%) and diammonium hydrogen phosphate $[(\text{NH}_4)_2\text{HPO}_4]$ (Sigma-Aldrich) (>98%) as starting materials and ammonia solution (30%) [Merck, India]. Synthesis of HAP was carried out by simple co-precipitation method involving mixing of calcium and phosphate precursors under constant stirring. The chemical reaction involving monobasic phosphate (equation 1) and dibasic phosphate (equation 2) reagents as phosphate precursors is given below [21]:



Looking at the reaction it becomes clear that the protons generated in the reaction lead to decrease the pH and consequently more bases is needed to neutralize the acid and maintain the reaction pH. The experimental procedure followed for preparation of HAP was same for both dibasic and monobasic phosphate precursors. The stoichiometric molar ratio for Ca:P is 1.67 in HAP. Taking the ratio into account, required amount of ammonium dihydrogen phosphate $[\text{NH}_4\text{H}_2\text{PO}_4]$ or diammonium hydrogen phosphate $[(\text{NH}_4)_2\text{HPO}_4]$ and calcium nitrate $[\text{Ca}(\text{NO}_3)_2 \cdot 4\text{H}_2\text{O}]$ calculated and dissolved in DI water. In a typical preparation of 10 g of HAP powder, 23.50741 gm. of calcium nitrate and 7.8876 gm. of diammonium phosphate was taken. Solutions of both, ammonium phosphate and calcium nitrate were prepared by adding 10 ml of water in to weighed reagents in a beaker. Ammonium hydroxide solution (13.6 M) was used as a pH regulator whose . To carry out the whole reaction in basic medium of pH 8 pH of ammonium phosphate was initially adjusted to 10 to 11. pH of ammonium phosphate solution was checked on regular interval until it reaches 10. Once pH reached to 10 we added rapidly calcium nitrate solution into ammonium phosphate solution. Through

course of the reaction pH was checked continuously. If pH was reducing more ammonium hydroxide solution was added. The pH was monitored next 45 to 60 minutes. Once pH became stable at 8 then it showed that reaction is completed. . Resultant white precipitate was left in basic medium for 24 hour. After aging the precipitate for 24 hour in basic medium, it was washed till neutral pH in order to get rid of excess of base and resultant soluble salt by-products. Washing was done by centrifuging the precipitate at 5000rpm for 3mins. Throwing away the supernatant and re-dispersing the settled precipitate in fresh DI water. This process was repeated 4-5 times till pH of the supernatant came to neutral. Resultant sample was dried in hot oven for 24 hours at 80°C. Sample was grinded for characterization by XRD. A schematic flow chart is presented below-

Flow Chart for the Synthesis of HAP:



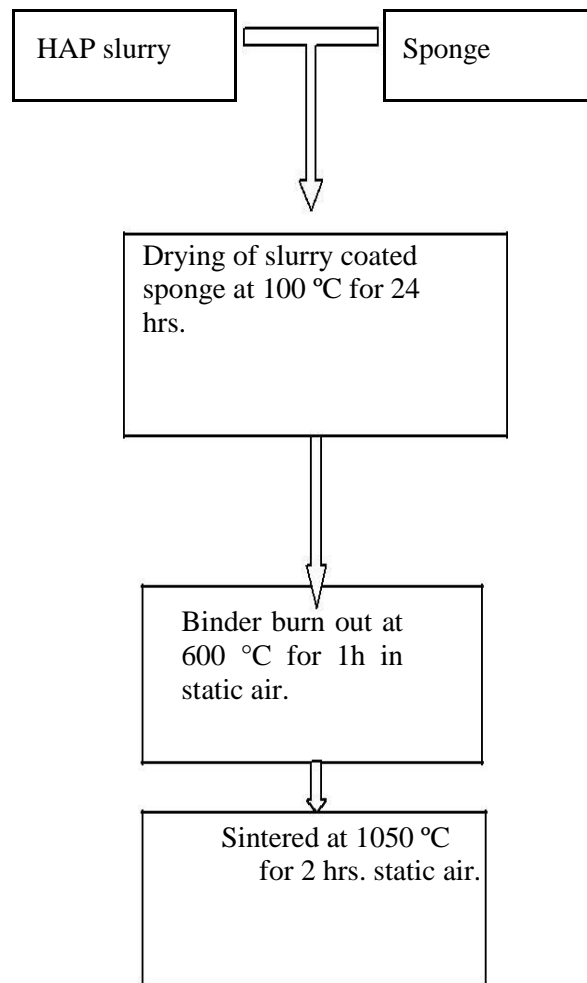
3.2. Preparation and optimization of slurry:

Once phase purity of HAP powders was confirmed from XRD, the phase pure powders were used for the preparation slurry. For the preparation of slurry various solvents such as De-ionized water, ethanol, acetone were tested in order to get desired coating of PU foams. Upon systematic study we found that water-ethanol mixture (volume ratio 50:50) was the most suitable solvent for preparation of slurry. As a binder 3 wt.% PVA was used. Traditionally, along with binders, other reagents are added as deflocculant, dispersant etc. However in our case, we did not need to use any such agents. The HAP slurry containing different weight percentage (35%,40 %,and 45 %) were prepared. Slurry was prepared by dispersing HAP powder in ethanol-water (50-50 vol%) solution of poly vinyl alcohol (PVA). The weight % of binder (PVA) to Powder (HAP) was 3% by weight.

3.3 Processing of porous HAP scaffolds through polymeric sponge method:

Scaffolds were prepared by the slurry dip-coating of polymer sponge followed by heat treatment at high temperature, in which at higher temperature PU foam burnt off and we get a 3-D structure of ceramic foam. Sponge pieces (approximately 1×1×1 cm) were pressed into the HAP slurry for impregnation. The soaked sponge was oven dried at 100 °C for 24 hours. The dried sponge was sintered at 1050 °C for 4 hour at a heating rate of 3 °C per minute. The samples were kept at 650 °C for one hour for binder and PU foam burn out. The sintered porous scaffold characterized for strength, porosity, pore size distribution, microstructure, in-vitro ageing tests etc. The process flow chart for fabrication of porous scaffold by polymeric sponge method was represented as:

Flow chart for fabrication of porous HAP scaffold by polymeric sponge method:



3.4 Mg-HAP composite preparation by melt casting of HAP scaffold by magnesium powder in an inert atmosphere:

Magnesium melt casting was tried in a tubular furnace in an inert atmosphere of argon/nitrogen. Scaffolds were kept in a cylindrical crucible covered by magnesium powder all around. The melt casting process was carried out at temperatures in the range of 750- 800 °C

3.5 Characterization:

3.5.1 Phase analysis of HAP nano powder, sintered HAP and magnesium (Mg):

Phase analysis was studied using the room temperature powder X-ray diffraction (Philips PAN analytical Netherland) with filtered 0.154056 nm Cu K α radiation. Samples are scanned in a continuous mode from 20°- 60° with a scanning rate of 0.04 (degree) / (sec). The HAP and Mg peaks were identified by referring JCPDS file (reference 74-0565). Particle size calculation by Debye-Scherrer equation:

$$\tau = \frac{K\lambda}{\beta \cos \theta} \quad (5)$$

Where:

- τ is the mean size of the ordered (crystalline) domains, which may be smaller or equal to the grain size;
- K is a dimensionless **shape factor**, with a value close to unity. The shape factor has a typical value of about 0.9, but varies with the actual shape of the crystallite;
- λ is the X-ray wavelength;
- β is the line broadening at half the maximum intensity (FWHM), after subtracting the instrumental line broadening, in radians. This quantity is also sometimes denoted as $\Delta(2\theta)$;
- θ is the Bragg angle.

3.5.2 Density and porosity measurement of HAP scaffold:

Density of porous scaffolds was measured by simply by measuring the weight and Length width and height of the scaffold. By calculating volumetric parameters we can calculate the volume of the scaffolds. Density of the scaffolds can be represented as:

$$\text{Porosity}(\%) = \left(1 - \frac{\rho_{\text{scaffold}}}{\rho_{\text{HAP}}}\right) \times 100 \quad (6)$$

ρ_{scaffold} - Density of scaffold

ρ_{HAP} - Density of HAP block

3.5.3 Measurement of wall thickness and pore diameter of scaffold:

As we know that strength properties all are depends on the thickness of the scaffold boundary. We also need controlled pore size of the not less than 100 μm . Wall thickness was calculated by with a simple optical microscopy. Where upper surface of the scaffold reflects the light and we gets an image of the upper surface. Exact view of the scaffold is given in results and discussions.

3.5.4 Compressive strength:

The compressive strength of the sintered samples was measured by universal testing machine (INSTRON 5966 10Kn load cell). Only rectangular and cubical scaffolds were used for the compression test and were broken in compression. The compressive strength of the pellets was determined from the following formula:

For cubic structure

$$\text{Compressive strength } (\sigma) = \frac{P}{A} \quad (7)$$

Where,

P= Load in kN

A= Cross sectional area of the cube

According to ASTM standards strength up to 10% of maximum load cell will be accurate. Whereas according to manufacturer's strength up to 1% of maximum load cell will be accurate. Here maximum load cell was 10 KN in our case.

3.5.5 Microstructure analysis by SEM:

Surface morphology, pore shape and pore size distribution was studied by SEM (Carl ZEISS SUPRAtm 40). The SEM images of gold coated sintered scaffold were observed in secondary electron ray at 10KV.

3.5.6 DSC of HAP-Mg Composite:

To know the phase change and melting point of different materials we used Differential Scanning Calorimetry (DSC). ASTM D3418 test was used for DSC. Differential Scanning Calorimetry is a thermos analytical technique in which the difference in the amount of heat required to increase the temperature of a sample and reference are measured as a function of temperature. Typical applications includes determination of melting point temperature, heat of melting, measurement of the glass transition temperature, curing and crystallization studies and identification of phase transformations.

3.5.7 Cell Culture test of scaffold:

For biocompatibility of scaffold cell culture test were performed. Adipose derived stem cells (ADSC) were isolated from the adipose tissue of a human donor. The scaffolds were washed for 4 days before the cells are seeded onto the scaffold. All the scaffolds were kept in vitro culture for one day.

Fluorescein diacetate (FDA) hydrolysis was used for the visualization of live cells. The viable cells metabolize the dye to a green fluorescent product, which was observed under a fluorescent microscope. In in vitro medium living cells converted non-fluorescent FDA into the green fluorescent compound. Fluorescein is a sign of viability. The red fluorescence by the dye propidium iodide (PI) is a signal that cells are not alive.

CHAPTER 4

Results and Discussion

4.1 Synthesis of HAP nano powders:

As mentioned in the experimental section HAP was synthesized by simple precipitation method. The molar ratio of Ca: P in hydroxyapatite is 1:1.67. Literature reports show that, not just the molar ratio but the pH conditions of the precipitation reaction is also important to obtain pure HAP phase [11]. In all the preparations the concentration of calcium and phosphate reagents was close to saturation limit. Two different types of phosphate precursors were used, mainly to observe the effect of precursors on phase formation of hydroxyapatite. In the first set of experiments, saturated solutions monobasic phosphate and calcium nitrate (Ca:P mole ratio of 1:1.67) were mixed together rapidly. The pH was adjusted in the range of 8-9 using ammonium hydroxides. We observed that precipitation process was rather slow and complete perception occurred over a period of 2 hours. XRD pattern of

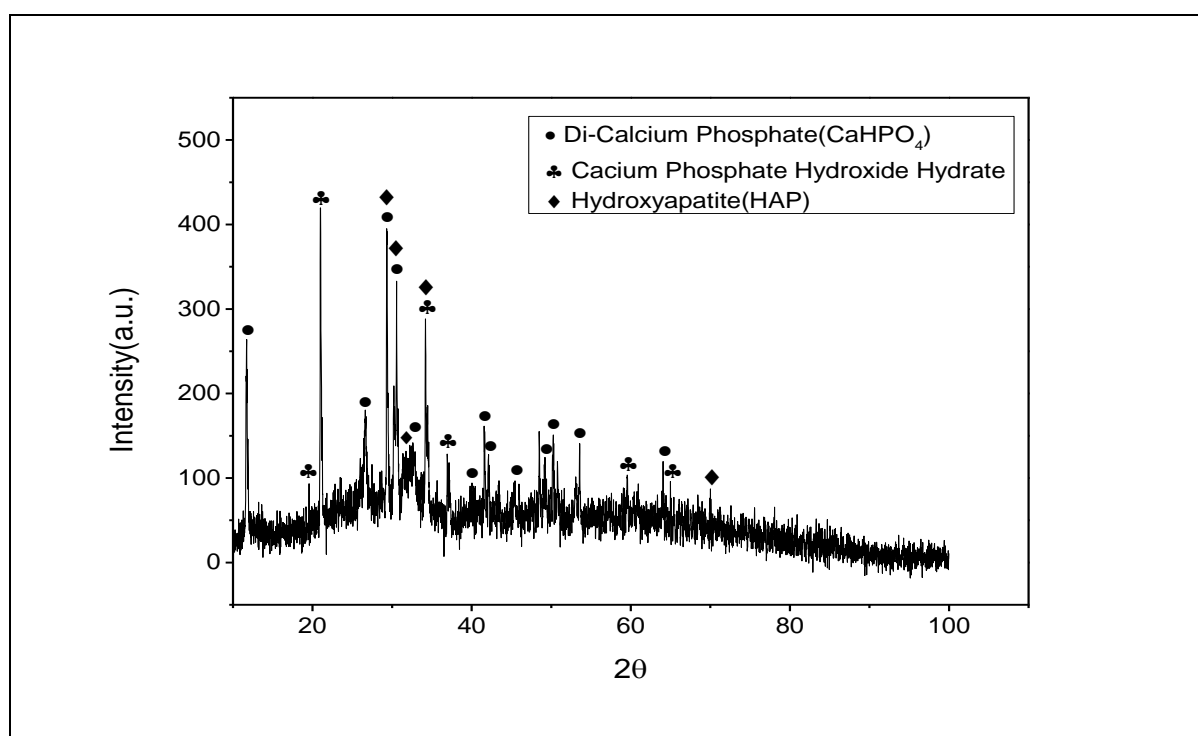


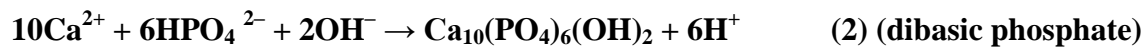
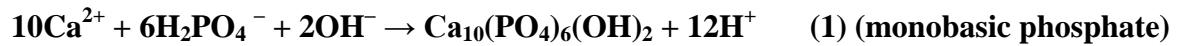
Fig 4.1 XRD pattern of HAP synthesized using monobasic phosphate as phosphate precursor.

resultant precipitate is shown in figure 4.1. peaks of di-calcium phosphate and calcium phosphate hydroxide hydrate. This may explained on the basis of the dissociation behaviour of the monobasic phosphate. In solution form of ammonium di-hydrogen phosphate dissociated weakly into ammonium ion and dihydrogen phosphate ions (Equation 1). As mentioned before, we used NH_4OH to adjust the pH of the solution. The addition of NH_4OH leads to increase in NH_4^+ ion concentration in solution.

Consequently, due to common ion effect the equilibrium in equation 1 gets shifted towards left resulting in decrease in free phosphate ions in the solution [19].



From this it follows that, though we mixed calcium and phosphate ions in 1:1.67 molar ratio, due to reaction conditions discussed above, the molar ratio of free calcium and phosphate ions was much lower in the solution. The low availability free phosphate ions was also evident from slow rate of precipitation. Secondly, recalling equation (1) & (2) in the experimental section,



From equation (1) & (2) it is clear that during precipitation, change in pH would be more in case of ammonium di-hydrogen phosphate compared to ammonium hydrogen phosphate. This necessitates addition of more NH_4OH to maintain pH. We believe that such drop transient drop in pH coupled with the deviation from stoichiometric molar ratio of Ca:P may have led to the formation of calcium phosphate phases other than HAP.

In the second set of experiments we used ammonium dihydrogen phosphate (dibasic phosphate) as a phosphate precursor. Reaction conditions were same as before. However in case of dihydrogen phosphate the precipitation occurred at much faster rate indicating greater concentration of free phosphate ions in the solution. As discussed above the change in pH was also less compared to monobasic phosphate. Effect of aging on phase was also tested Fig-4.2 shows the XRD pattern of as-prepared by co-precipitation method with and without aging in basic medium. In both cases all the peaks matching with standard XRD pattern of HAP were seen. The broad nature of diffraction peaks indicates that the resultant powders were nanocrystalline. Though, no additional or impurity phase were seen in the XRD pattern presence of amorphous calcium phosphate cannot be denied. As evident from XRD pattern, the baselines for both freshly precipitated and aged sample is not flat but show two broad humps in 2θ range of 20° - 40° and 40° - 70° . XRD patterns with such broad humps have been reported for amorphous calcium phosphate [22]. Presence of these broad humps suggest that there may be short range ordering present between calcium and phosphate ions.

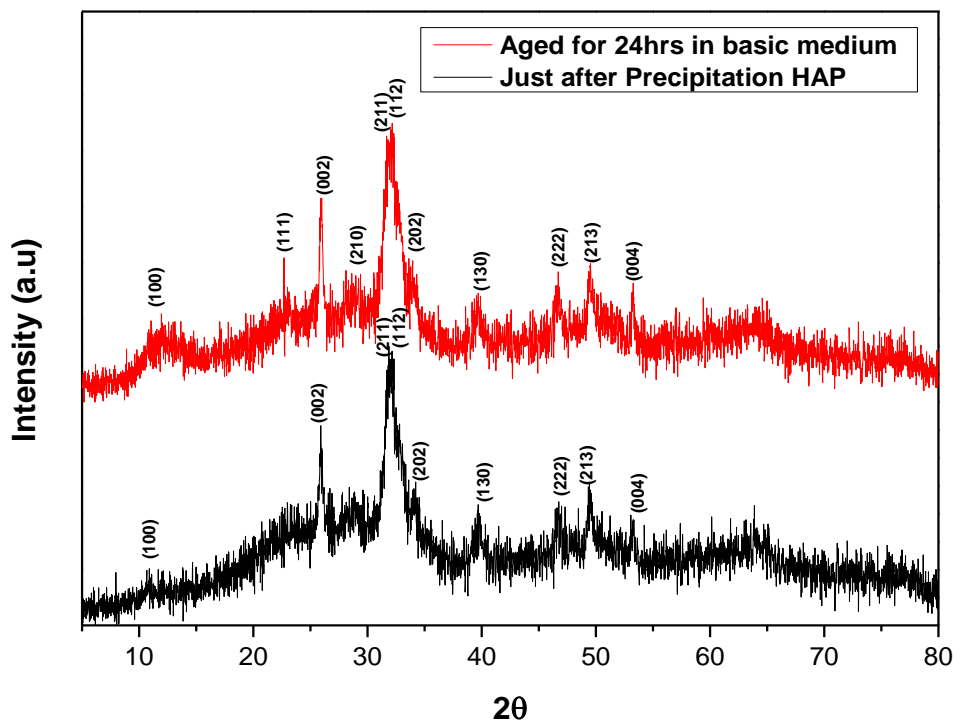


Fig 4.2: XRD pattern of HAP just after precipitation and aged after keeping in basic medium for 24 hrs.

Using the standard data file of HAP (JCPDS files #721243) the peaks were indexed as shown in figure 4.2. The crystallite size was calculated from (002) using the Debye-Scherrer equation. The crystallite size of as-prepared sample and sample aged in basic medium was 21 nm and 24 nm respectively. This shows that with aging crystallinity of the samples improves slightly. Thus in case of calcium phosphate powders prepared using dibasic phosphate precursor yielded nano crystalline HAP powders.

4.2 Optimization of slurry preparation

Traditionally, for the preparation of ceramic slurry, ceramic powders with particles having size in the range of microns. Typically, along with binders, other reagents are added as deflocculant, dispersant etc. however in our case, our starting powders had particle size in nano range and powders were quite free flowing and agglomeration free figure 4.3.

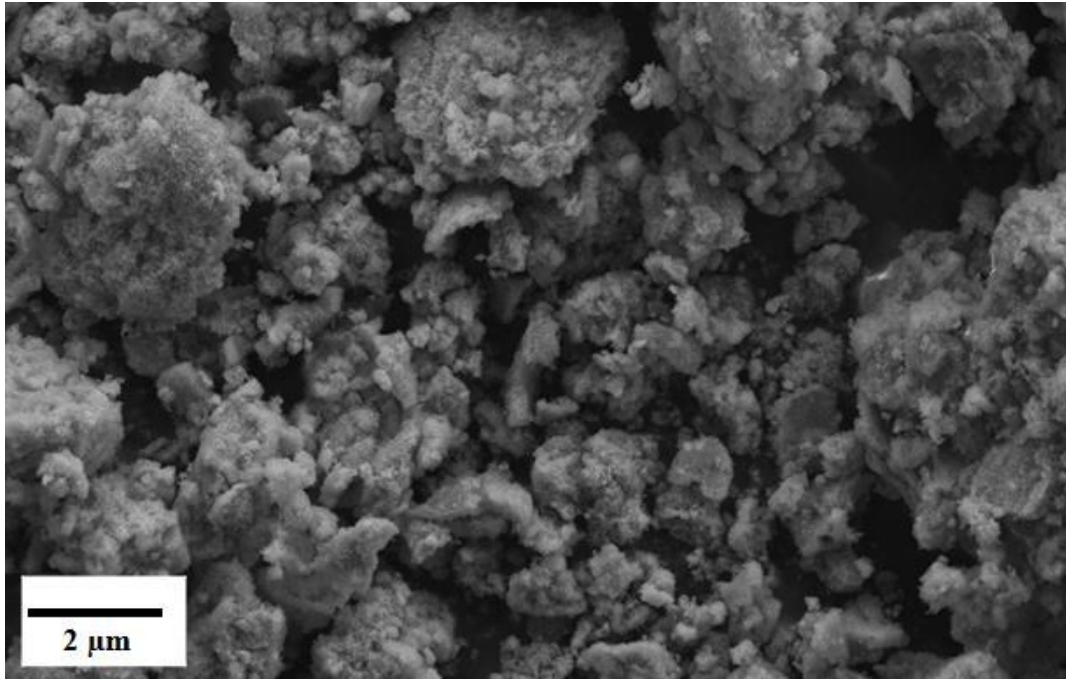


Fig. 4.3 SEM image of Nano powder synthesized by co-precipitation method.

Consequently, addition of deflocculant, dispersant etc. was not needed in our case. PVA was used both as binder as well as deflocculant and dispersant. In order to get slurry with optimum properties such as viscosity, wettability of PU foam etc., we tried multiple solvent systems. Firstly, we used DI water for the preparation of slurry but that was not suitable for coating as bubbles were forming during processing of foam which seems to block pores in the PU foam and restrict proper coating of interior pore. . So to restrict from bubble formation we used many solvents including acetone and ethanol. Acetone was not suitable due to its high evaporation rate concentration of the slurry could not be maintained over the period of coating process. Due to fast evaporation rates an even coating could also be seen. Finally, 50:50 volume % of water/ethanol solvent system was used. Which seems to work well in terms of coating of PU foams as we were able to get almost bubble-free slurry-coated PU foams and the evaporation rate of the solvent system was not very rapid therefore even coating could be observed. For all further experiments HAP slurry with 50:50 volume % water-ethanol solvent mixture was used.

4.3 Phase analysis of HAP after sintering:

The XRD pattern in fig 4.4 shows that the calcined powder contains only hydroxyapatite (HAP), tri-calcium phosphate (TCP) (impurity) and calcium hydrogen phosphate (impurity) peaks. As discussed earlier, though the XRD pattern of as-synthesized powders showed peaks corresponding to HAP the uneven baseline suggested the presence of amorphous calcium phosphate. In addition, the HAP preparation was not carried out in a CO₂ free atmosphere due to which CO₃²⁻ doping in HAP cannot be avoided. Such doping leads to the formation of calcium-deficient HAP which upon heat treatment results

in phase segregation. We believe that the impurity phases seen in XRD pattern of sintered sample may be due one or all of these reasons mentioned above.

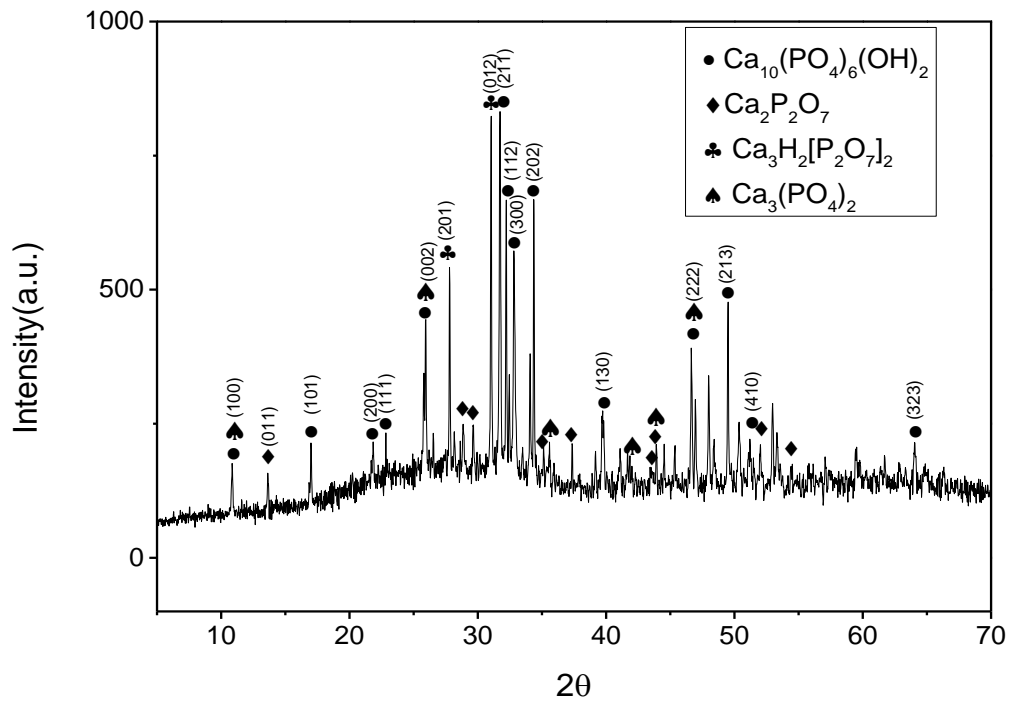


Fig. 4.4 XRD curve of Sintered HAP scaffold at 1000 °C

4.4 Phase analysis and DSC and XRD curve of Mg before and after heat treatment :

XRD pattern showed that magnesium have pure phase before heat treatment without any impurity. Major peaks assigned to pure Mg.(100) (002) and (101) confirms there phase purity. However in second graph of heat treated magnesium they are showing peaks of Mg but presence of MgO is also detected. (200) and (220) planes are the peaks of Magnesium oxide. Magnesium oxide may be preventing merging of molten magnesium droplets by covering outer surface of the magnesium powder. Thus for the synthesis of HAP-Mg composite we need a very high quality inert atmosphere where we can give sufficient time to Mg so that they can travel through the channels of the scaffold.

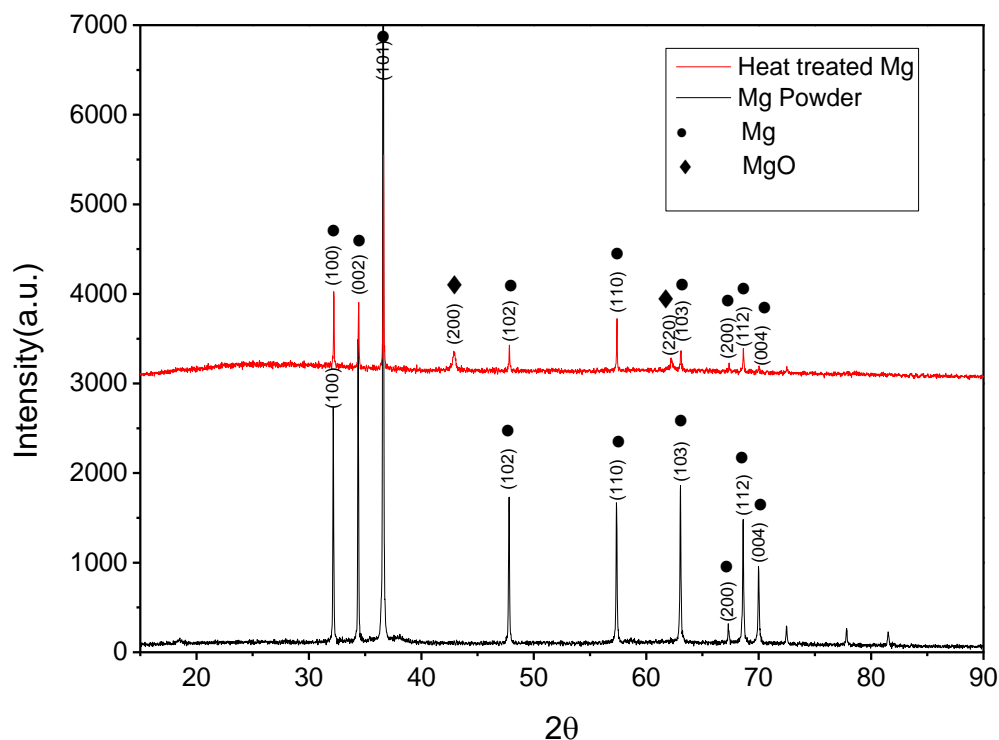


Fig. 4.5 XRD pattern of magnesium and heat treated magnesium after melting (JCPDS 04-0770)

The phase purity and presence of other oxides was evaluated from thermal analysis. In figure 4.6 DSC was done to know melting point and purity of magnesium powder. As it is shown for Mg granular at 656.3°C an endothermic sharp peak is there which confirms melting point of magnesium. Since no other peaks were found, hence it was confirmed that magnesium was pure and ideal for the Composite.

Fig. 4.6 showed DSC characterization of magnesium powder after heat treatment as we already seen in the XRD pattern that some impurity entered into the system after heat treatment. Here we analysed three points. For these temperatures are 616 °C, 626 °C and 651.2 °C respectively. Since we processed this magnesium with HAP, an additional weight loss occurred upon further heating up to 600 °C following a strong exothermic peak at ~616 °C. This loss was attributed to the removal from the surface (ammonium and water) and the lattice (water and carbonate).

Here in the fig 4.6 we can compare changes in the heat flow at different temperature ranges. It clearly showed that without high purity inert gas and inert atmosphere melting of the magnesium leads to magnesium oxide, which prevents the formation of Mg-HAP composite. Due to the formation of MgO oxide in the crucible magnesium oxide covering the Mg powder and restricting merging of molten droplets to form molten mass which can successively infiltrate HAP scaffold and form Mg-HAP composite.

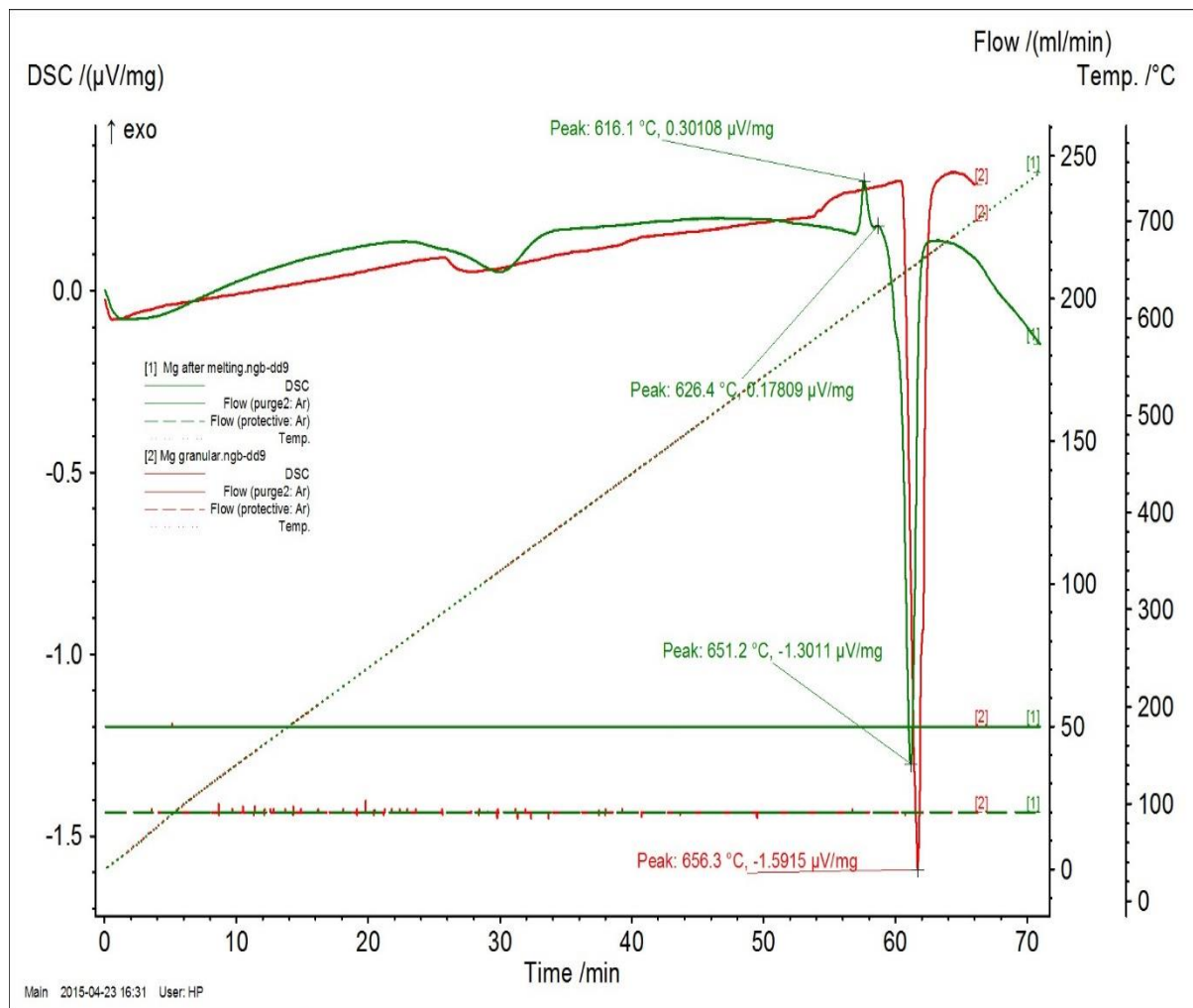


Fig. 4.6 DSC curve for comparative study of heat treated and simple magnesium powder heated at a rate of 10 °C/min.

4.5 Density and porosity measurement:

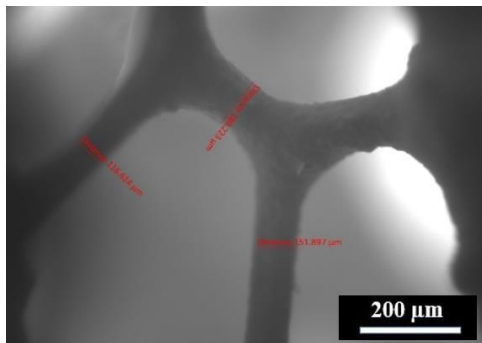
The effect of HAP concentration on the wall thickness and density of HAP scaffold is shown in Table-4.1. This table indicates that for different concentration of HAP wall thickness and Density varies directly proportional to concentration. Simply we can conclude for higher concentration coating is done well than lower one. Similarly sample having higher concentration are more dense compare to lower one. This is due to the fact that increasing the HAP amount causes grater gel formation which increases the strength of green body which turn increases the fired strength.

Table 4.1 showing density and porosity of different loading percentage:

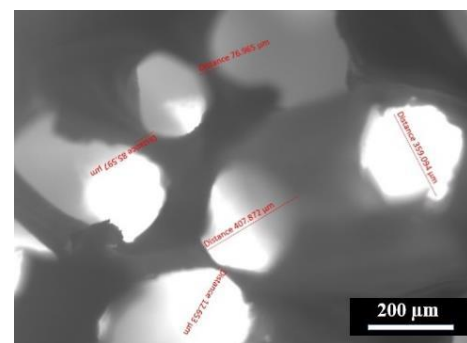
HAP %	Foam Used(ppi)	Volume of Scaffold	Weight of Scaffold	Density(avg.) Min. 3 scaffold	Porosity %
35 %	60 ppi	0.231 cc ³	0.0596 gm.	0.244 gm/cc ³	93.38
40 %	60 ppi	0.45 cc ³	0.0935 gm	0.2777 gm/cc ³	91.78
45 %	60ppi	0.40 cc ³	0.1684 gm	0.421 gm/cc ³	86.59
35 %	30 ppi	2.88 cc ³	0.6230 gm	0.2205 gm/cc ³	93.11
40 %	30 ppi	1.68 cc ³	0.4569 gm	0.288 gm/cc ³	91.338
45 %	30ppi	1 cc ³	0.3870 gm	0.3870 gm/cc ³	87.67

4.6 Wall thickness and microstructure (SEM):

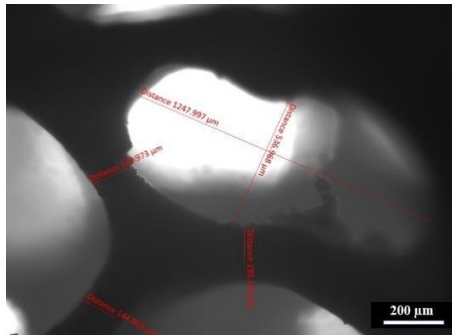
Waal thickness and Pore size were calculated with the help optical microscopy. However due to large size of scaffold we cannot take image of whole sample. Particular wall and Pore is taken here for analysis. Since we need minimum 100 µm pore hence pore sizes are bigger enough than minimum requirement. These are images of scaffolds with different loading concentrations. Below are given optical images of scaffolds of different concentrations-



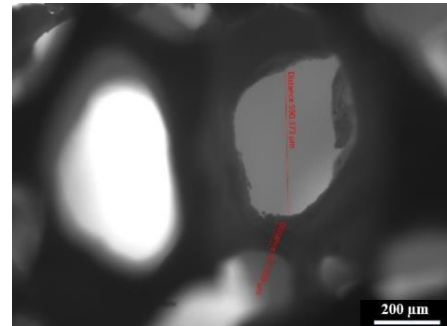
(i) 35 wt. % of HAP and 30 ppi



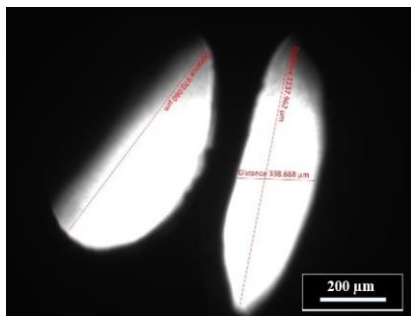
(ii) 35 wt. % of HAP and 60ppi



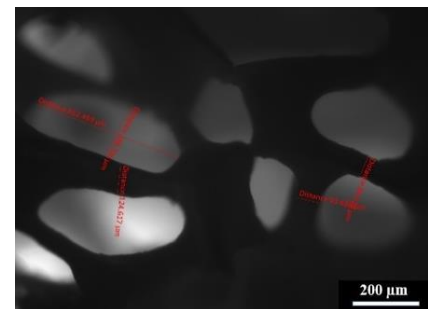
(iii) 40 wt. % of HAP and 30ppi



(iv) 40 wt. % of HAP and 60ppi



(v) 45 wt. % of HAP and 30 ppi



(vi) 45 wt. % of HAP and 60 ppi

Fig. 4.7 Optical microscopy images of HAP scaffold (magnification 50x).

Table 4.2 Showing average wall thickness and pore diameter of different HAP concentrations.

Wt. % of HAP	Foam Used (ppi)	Wall thickness of scaffold (μm)	Pore Diameter (μm)
35 %	60 ppi	75.145	573.1492
40 %	60 ppi	101.6507	436.100
45%	60 ppi	157.502	426.9778
35 %	30 ppi	167.200	903.704
40 %	30 ppi	181.606	891.608
45 %	30 ppi	264.4625	698.5982

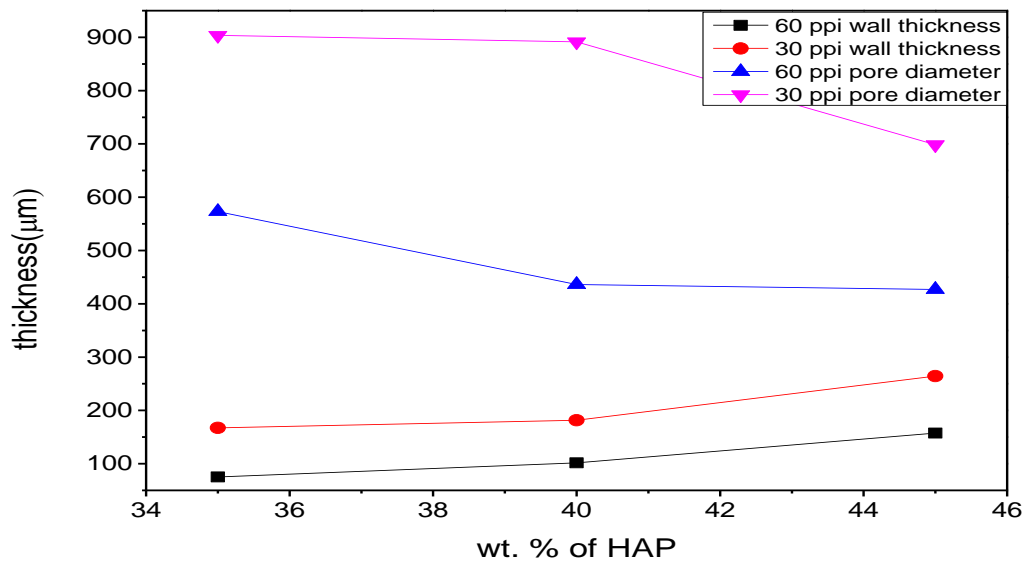


Fig. 4.8 Wall and diameter thickness Vs. wt. % of HAP

Scaffolds prepared by polymeric sponge method where 30 ppi and 60 ppi sponges were used for the coating of slurry sintered at 1000 °C.

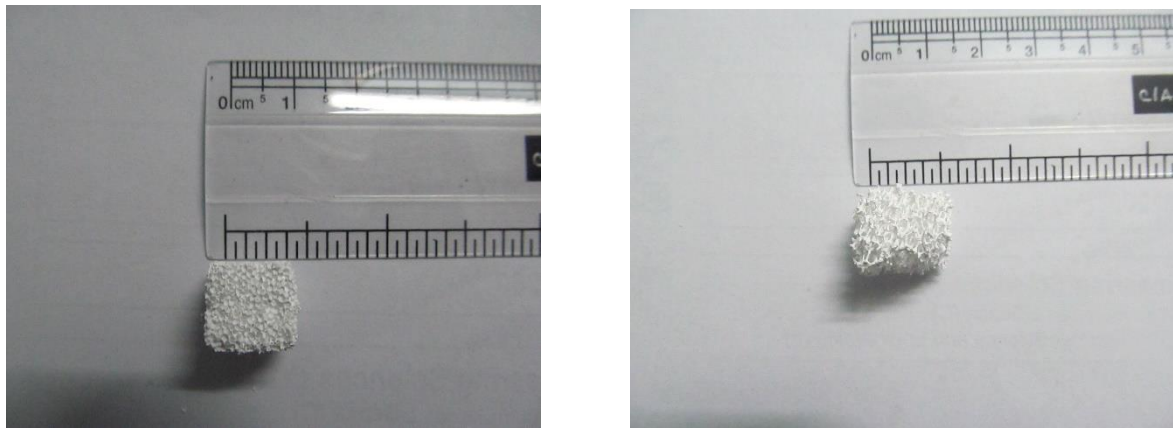


Fig- 4.9 Sintered hydroxyapatite scaffold prepared by polymeric sponge method.

Fig -4.10 shows the SEM images of porous HAP scaffolds prepared from polymeric sponge method with varying HAP and PVA contents. It has been seen that macro-pore were inter connected through cell walls. Pores were well connected and walls were not damaged due to PU evaporation. The SEM images are shown as:

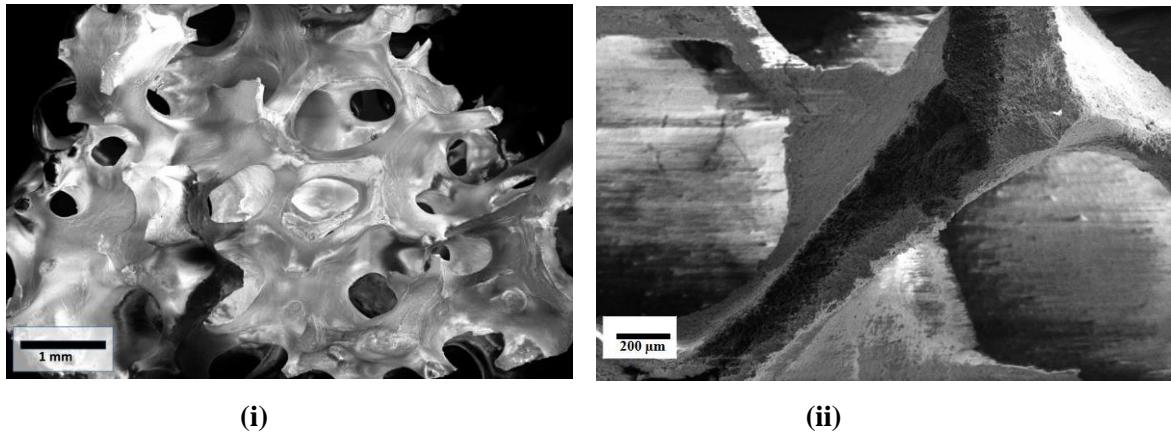


Fig- 4.10 SEM image of HAP scaffolds prepared from polymeric sponge method with 40% HAP content (i) Image of scaffold with pores (ii) Image of scaffold walls.

From the SEM image it was observed that pores were well interconnected. The concentration of HAP affect the pore size, porosity, pore inter connectivity as well as strength of scaffold. Image 4.10 (i) has well interconnected pores with pore diameter 300~700 μm .

We did not used SEM for the measurement of wall thickness and pore diameter because SEM was not in working condition. All images of scaffold from SEM taken at last moment. Even after correction of SEM there was chance of sucking HAP powder by vacuum pump hence we used only a few scaffolds for the image.

4.7 Compressive Strength:

It has been observed that with increasing HAP contents from 35% to 45% porosity decreases whereas compressive strength increases in HAP scaffolds. Here we observed that strength of scaffold also depends on sintering temperature. In the figure it has been observed that compressive strength decreases from 0.0065 MPa to 0.00432 MPa in 60 ppi foam when HAP concentration changes from 45% to 35%. Similarly compressive strength of scaffold with 30 ppi decreases from 0.0125 MPa to 0.00795 MPa on decreasing concentration of HAP from 45% to 35%. However scaffolds synthesized by 30 ppi foams have greater compressive strength than scaffolds which were synthesized by 60 ppi foam when compared at fixed concentration of HAP.

Table 4.3 Showing average porosity and compressive strength of different HAP concentrations.

HAP %	Foam Used	Porosity %	Compressive strength(MPa)
35	60 ppi	93.38	0.00432
40	60 ppi	91.78	0.0058
45	60 ppi	86.59	0.0065
35	30 ppi	93.11	0.00795
40	30 ppi	91.338	0.00914
45	30 ppi	87.67	0.0125

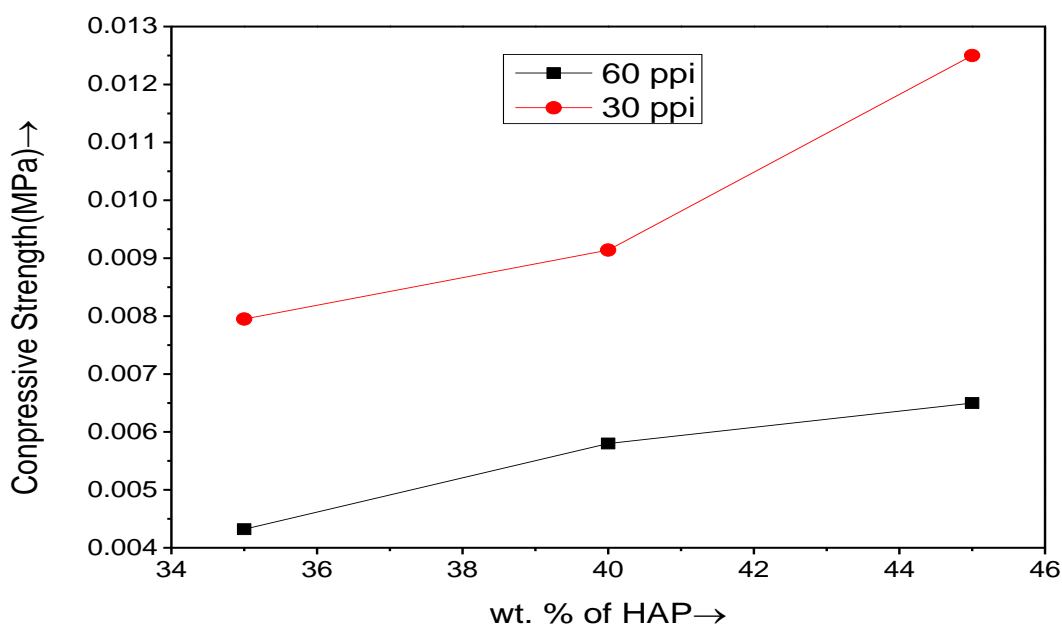


Fig. 4.11 Compressive strength of HAP scaffold Vs. wt. % of HAP in the slurry used for foam coating

4.8 Cell Culture test of scaffolds:

As we can conclude from the figure 4.12 that no or very less number of red fluorescence were found, this confirms that they were alive and were healthy. Medium with scaffold was suitable for cells.

It was observed that cells adhered to the scaffolds and were healthy, which confirms growth of the cells. After one-day in culture medium many cells were alive adhered with HAP. Hence material was considered to be bio-compatible.

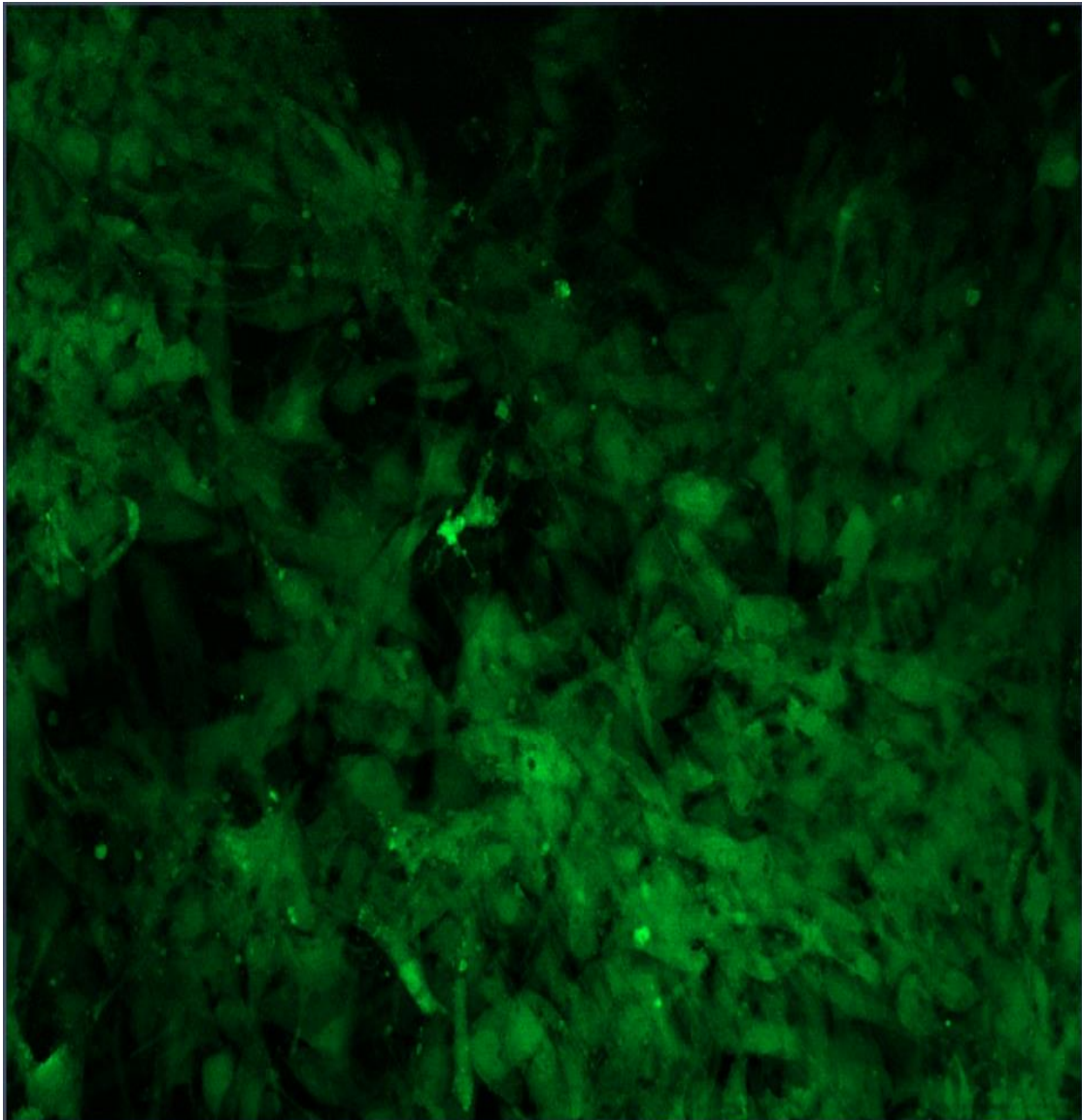


Fig. 4.12 Florescence microscopy images of scaffolds seeded with adipose derived stem cells.

In the culture medium there were a lot of particles fallen from scaffolds, this was due to improper packing and sintering of the HAP. We sintered the sample at 1050°C , where as in papers peoples went up to 1250°C . Hence improper sintering temperature also affects strength of the scaffolds.

CHAPTER 5

CONCLUSION

Conclusions:

- HAP prepared by $\text{Ca}(\text{NO}_3)_2 \cdot 4\text{H}_2\text{O}$ and $\text{NH}_4\text{H}_2\text{PO}_4$ was not phase pure and contained impurities such as calcium hydrogen phosphate (DCP).
- The HAP prepared from $\text{Ca}(\text{NO}_3)_2 \cdot 4\text{H}_2\text{O}$ and $(\text{NH}_4)_2\text{HPO}_4$ by co-precipitation method was in phase. However, with possible doping of carbonate ions presence of amorphous calcium phosphate pure.
- The porous scaffolds were prepared from polymeric sponge method. Porous HAP prepared from polymeric sponge method had about 85-90% porosity having pore diameter $\sim 300\text{-}900\ \mu\text{m}$ and the pores were well inter-connected.
- Increasing PVA content can lead to bubble formation in HAP slurry hence 3% was ideal condition for sponge coating. In addition water-ethanol 50:50 vol% mixed solvent system was helpful in preventing bubble formation and maintaining slurry consistency.
- With increase in HAP contents by 5 wt.% with solid loading, the strength of scaffold also increases.
- The pore size and pore inter connectivity depended upon the slurry viscosity and solid Loading.
- On increasing HAP content by 5% wall thickness and density of the scaffold increases proportionally.
- Pore connectivity also depends on the PU foam used for synthesis of scaffold, large pore diameter have maximum chance of mechanical failure than smaller pore diameter.
- On SEM analysis it was clear that all the pores were connected properly.
- Magnesium melting was affected by possible oxygen impurity present in the inert gases and tubular furnace, hence was not melted properly. Traces of magnesium oxide were seen along with pure magnesium metal in heat treated samples.

Future Plan:

In the current work we were unable to synthesize Mg-HAP composite due to frequent oxidation and time limitation of the project. However we collected a lot of information about the composite. For the solid composite (HAP-Mg) we must be very careful during heat treatment of magnesium with HAP. Inert gases used for melting of the magnesium must be 100% pure.

Magnesium-HAP can be revolutionary for hip implant and other bio-material application. HAP-Mg composite is providing most bio-compatible material for hip replacement and after completing their objectives finally they will degrade.

References:

- [1] <http://www.doitpoms.ac.uk/tlplib/bones/printall.php>.
- [2] J. J. Jacobs, J. L. Gilbert, R.M. Urban. Current concepts review-corrosion of metal orthopaedic implants. *J. Bone Joint Surg. Am.* 80-A (2), (1998) 268- 282.
- [3] F. Matassi, A. Botti, L. Sirleo, C. Carulli and M. Innocenti. Porous metal for orthopaedics implant. *Clin. Cases Miner Bone Metab.* 10(2), (2013) 111-115.
- [4] J.E. Lang, D.R. Whiddon, E.L. Smith, A.K. Salyapongse. *J Surg Orthop Adv.* 17(1), (2008) 51-57.
- [5] V. Karageorgiou and D. Kaplan. Porosity of 3D biomaterial scaffolds and osteogenesis. *Biomaterials* 26, (2005) 5474–5491.
- [6] D. Veiqi, P. Vavrik, D. Pokorny, M. Slouf, E. Pavlova, I. Landor. Comparison of in vivo Characteristics of polyethylene wear particles produced by a metal and ceramic femoral component in total knee replacement. *Acta Chir Orthop. Traumatol Cech* 78(1), (2011) 49-55.
- [7] I. Nakahara, M. Takao, S. Bandoh, N. Bertollo, W.R. Walsh, N. Suqano. In vivo implant fixation of carbon fibre reinforced PEEK hip prostheses in an ovine model. *J. Ortho. Res.* 31(3), (2013) 485-92.
- [8] E. Erkmén, G. Meriç, A. Kurt, Y. Tunc, A. Eser. Biomechanical comparison of implant retained fixed partial denture with fibre reinforced composite versus conventional metal frameworks : A 3D FEA study. *Journal of the Mechanical Behavior of Biomedical Materials*, 4(1), (2011) 107- 116.
- [9] H. S. Brar, M. O Platt, M. Sarntinoranont, P. I. Martin, M. V. Manuel. Magnesium as a biodegradable and bioabsorbable material for medical implant. *JOM* 61(6), (2009) 31-34.
- [10] J.C. Middleton, A.J. Tipton. Synthetic biodegradable polymers as orthopaedic devices. *Biomaterials* 21,(2000) 2335-2346
- [11] M.P. Staiger, A.M. Pietak, J. Huadmai, G. Dias. Magnesium and its alloys as orthopaedic biomaterials: A review. *Biomaterials* 27(9), (2006) 1728-1734.

- [12] A. Cuneýt Tas. Synthesis of biomimetic Ca-hydroxyapatite powders at 370C in synthetic body fluids. *Biomaterials* 21, (2000) 1429-1438.
- [13] R. Palanevelu, A Mary Saral, A. Ruban Kumar. Nano crystalline hydroxyapatite prepared under various pH conditions. *Spectrochimica Acta Part A: Molecular and Biomolecular Spectroscopy*, 131, (2014) 37-41.
- [14] S. H. Kwon, Y. K. Jun, S.H. Hong, I. S. Lee, and H.E. Kim. Calcium phosphate bioceramics with various porosities and dissolution rate. *J. Am Ceram. Soc.*, 85(12), (2002) 3129-31.
- [15] I. Sopyan, M. Mel, S. Ramesh, and K.A. Khalid. Porous hydroxyapatite for artificial bone applications. *Sci. Tech. Adv. Mater.* 8, (2007) 116-123.
- [16] H.R. Ramay and M. Zhang. Biphasic calcium phosphate nanocomposite porous scaffolds for load bearing bone tissue engineering. *Biomaterials* 25(21), (2004) 5171- 80
- [17] V. Karageorgiou and D. Kaplan. Porosity of 3D biomaterial scaffolds and Osteogenesis. *Biomaterials* 26, (2005) 5474–5491.
- [18] K. Schwartzwalder and A. V. Sommers, US patent No. 3090094, may 21 (1963).
- [19] X. N. Gu, W.R. Zhou, Y.F. Zheng, Y.Liu and Y.X. Li . Degradation and cytotoxicity Of lotus type porous pure magnesium as potential tissue engineering scaffold *Materials Letter* 64(17), (2010) 1871-1874.
- [20] B. Denkena and A. lucas, Biocompatible magnesium alloys as absorbable implant materials-adjusted surface and subsurface properties by machining process *CIRP Annals- Manufacturing Technology* 56(1), (2007)113-116.
- [21] H. Eslami, M. Solati-Hashjin, F. Bakhshi. Synthesis and characterization of nanocrystalline hydroxyapatite obtained by the wet chemical technique. *Materials Science Poland* 28(1), (2010) 5-13.
- [22] A. L. Boskey. Amorphous calcium phosphate: the contention of bone. *J Dent res* 76, (1991) 1433-1436.
- [23] <http://www.chemspider.com/Chemical-Structure.22812.html>
- [24] <http://en.wikipedia.org/wiki/Hydroxylapatite>.

